Optics Communications 85 (1991) 326–330
North-Holland

OPTICS
COMMUNICATIONS

Measurement of background energy content of a linear cw colliding pulse mode-locked dye laser

W. Bäumler and A. Penzkofer
Naturwissenschaftliche Fakultät II-Physik, Universität Regensburg, W-8400 Regensburg, Germany

Received 1 February 1991; revised manuscript received 20 June 1991

The background energy content of a linear cw CPM rhodamine 6G-DODCI femtosecond dye laser is determined by time-resolved measurement of the Rayleigh scattered signal in a colloidal silicon dioxid suspension with an ungated inverse time-correlated single photon counting system. A constant background intensity signal is observed outside the temporal region of the instrument response function of the detection system. Assuming the same background intensity level within the temporal region of the instrument response function, an average background intensity level of approximately 2.5×10^{-8} of the peak pulse intensity, and a background energy content of approximately 2×10^{-3} of the pulse energy are found.

1. Introduction

The background energy content between the pulses of a mode-locked laser is a measure of the mode-locking quality. It reduces the resolution in time-resolved spectroscopic measurements. For intense pulsed picosecond lasers various techniques have been applied to determine the background energy content [1–14] (overexposed photodetectors [1,2], photo-conductivity of silicon switches [3,4], contrast ratio of two-photon fluorescence traces [2,5], efficiency of third harmonic generation [6,7] and three-photon fluorescence [2,8], parametric four-photon interaction [9,10], frequency mixing of fundamental and second harmonic light [11], streak camera measurements [12], and saturable absorption [13,14]). For cw mode-locked picosecond and femto-second lasers [15–18] no detailed background energy content measurements have been reported yet.

In this paper the temporal background intensity distribution and the background energy content of a linear cw colliding pulse mode-locked femtosecond dye laser [15–18] is determined by time-resolved measurement of the signal of a Rayleigh scatterer (Ludox CL-X) with an ungated inverse time-correlated single photon counting system [19,20].

For the signal analysis the same background intensity level is assumed within the instrument response region of the detection system as in the time-resolved region. Without this assumption an upper background intensity limit within the instrument response region is estimated from non-collinear second harmonic generation autocorrelation traces [18].

2. Experimental

The experimental setup of the cw linear colliding pulse mode-locked (CPM) dye laser system [17] and of the inverse time-correlated single photon counting system [19,20] is depicted in fig. 1. The CPM laser is pumped by the multimode emission of a cw argon ion laser including the 488 nm and 514.5 nm lines (Spectra-Physics Model 2016, 3 watt power applied). The gain medium is rhodamine 6G in ethylene glycol (3×10^{-3} molar, jet thickness 250 μm, flow velocity 2.8 ms^{-1}) and the saturable absorber medium is DODCI (3,3′-diethyloxadicarbocyanine iodide) in ethylene glycol (3.5×10^{-4} molar, jet thickness 35 μm, flow velocity 7 ms^{-1}). The saturable absorber jet is placed in the center of the resonator to achieve temporal overlap of the counter-propagating pulses in the absorber jet (colliding pulse mode-locking). The resonator length is 2.5 m leading to a pulse separation of 8.3 ns. A parallel prism

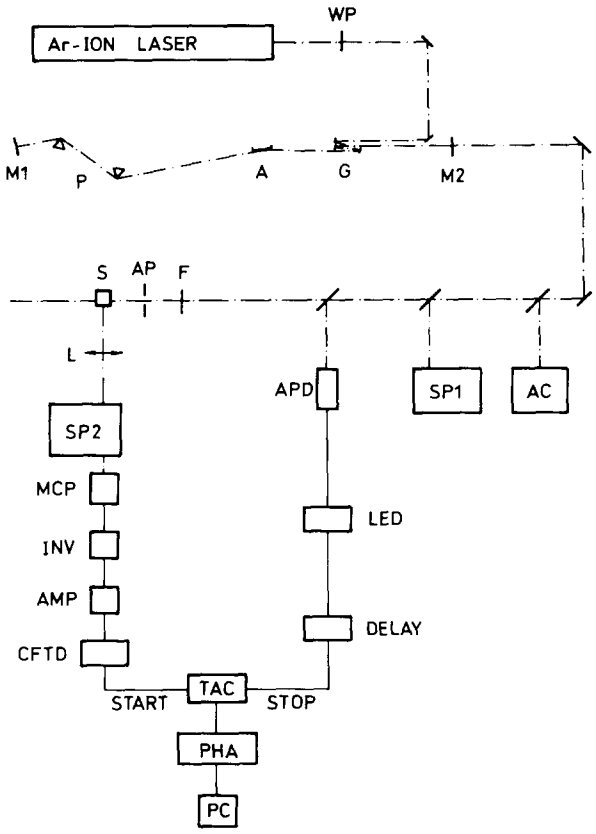

Fig. 1. Experimental setup. WP, $\lambda/2$ wave plate. M1, high reflectivity broadband single-stack mirror. M2, single-stack output mirror with reflectivity $R=0.97$. G, gain cavity with mirror curvatures $\rho=10$ cm, jet thickness 250 μm (position at one quarter of resonator length). A, absorber cavity with mirror curvatures $\rho=5$ cm, jet chickness 35 μm (position exactly at one half of resonator length). P, prism pair, AC, intensity autocorrelator [24], SP1, SP3, grating spectrometers. F, interference filter. AP, aperture. S, sample containing Ludox CL-X. L, lens. MCP microchannel plate photomultiplier (Hamamatsu R1564-01, voltage −2900 V). INV, inverting transformer (EG&G IT 100). AMP, 25 dB broadband amplifier (Minicircuits ZL-1042 J, 10 MHz–4.2 GHz). APD avalanche photodiode (Telefunken BPW28). CFTD, constant-fraction time discriminator (Tennelec TC454 with fraction module $f=0.2$). DELAY, coaxial cable delay box (Ortec model 425 A). TAC, biased time to pulse height converter (Ortec model 457) adjusted to 130 channels per ns, PHA, pulse height analyser multichannel analyser system (Ortec Norland 5608). PC, personal computer.

pair (prism distance 30 cm, fused silica Brewster angle prisms) is inserted for compensation of group velocity dispersion and chirped pulse compression [21–23].

The pulse spectra are monitored with a grating spectrometer SP1 and a vidicon system. The laser-wavelength is $\lambda_L \approx 620$ nm. The pulse durations are measured with a rotating mirror intensity autocorrelator applying a noncollinear phasematched second harmonic KDP crystal [24]. Pulse durations down to 50 fs have been obtained by fine adjustment of the prism positions and the jet positions. In the experiments described here the pulse durations were $\Delta t_L \simeq 90$ fs.

The time-correlated single-photon counting system is operated in an ungated inverse mode (single photon signals start time-to-amplitude converter). The full 120 MHz pulse repetition rate of the CPM laser is applied. The components of the single photon counting system are listed in the caption of fig. 1. The sample cell contains a colloidal silicon dioxid suspension in water (Ludox CL-X from DuPont, particle size 21 nm, undiluted scattering coefficient at 620 nm is 0.2 cm^{-1} [25]). In fluorescence decay studies this suspension is used for recording the instrument response function of the system. The single photon detector is a fast microchannel plate photomultiplier tube (Hamamatsu type R1564-01, microchannel diameters are 12 μm) and the trigger detector is a fast avalanche photodiode (Telefunken BPW28). The Rayleigh scattered signal $S(t)$ and the photomultiplier noise signal $S_u(t)$ are measured separately and the noise signal is subtracted to obtain the true Rayleigh scattering signal $S_0(t)=S(t)-S_u(t)$. An analysis of $S_0(t)$ delivers the background intensity and energy contents.

3. Results

The Rayleigh scattering signal is recorded and analysed by assuming a constant background light distribution. Additionally an upper limit of the background intensity level within the instrument response width is estimated by analysing noncollinear phasematched second harmonic generation autocorrelation traces.

3.1. Rayleigh scattering trace

The Rayleigh scattered signal $S(t)$ was accumulated over a time period of 3 hours. The number of

counts in the channel of maximum counts was nearly 2×10^6. The total number of counts summed over all channels was approximately 6.45×10^7. The microchannel plate photomultiplier noise signal $S_u(t)$ was accumulated over the same time period, where half of the measurement was done before and the other half after the Rayleigh scattering measurement. For the noise signal measurement the entrance to the spectrometer SP2 was covered. The noise signal was rather constant over the channels. The average noise signal height was the same in the accumulation before and after the Rayleigh scattering measurement. The total accumulated average number of noise counts per channel was 290.

The dark-noise corrected and normalized Rayleigh scattering signal $S_n(t)=S_0(t)/S_{0,max}$ is displayed in fig. 2 $[S_0(t)=S(t)-S_u(t)]$. It consists of an intense pulse extending from t_{pb} to t_{pe}, two weak pulses at t_{a1} and t_{a2}, and a rather constant pedestal

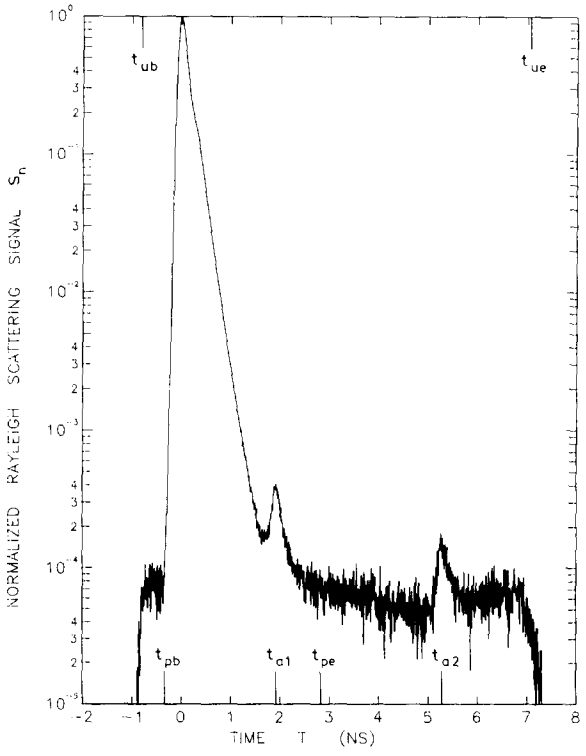

Fig. 2. Normalized Rayleigh scattering signal versus time. Signal detection is limited to time separation between adjacent pulses (longest delay between start and stop pulse is pulse separation $T=8.3$ ns).

from t_{ub} to t_{ue}. The intense signal pulse has a full halfwidth of 180 ps characterizing the instrument response time. The signal pulse extension from t_{pb} to t_{pe} is caused mainly by the transit time spread of photoelectrons in the microchannel plate photomultiplier (MCP) and the timing jitter of the constant fraction time discriminator (CFTD) and the leading edge discriminator (LED). The true signal duration is equal to the CPM laser pulse duration ($\Delta t_L \approx$ 90 fs). The two weak pulses at t_{a1} and t_{a2} are most likely after-pulses of the MCP photomultiplier. They are not due to satellite pulses of the CPM laser because there are no optical components at appropriate timing positions in the resonator. The pedestal signal is thought to be Rayleigh scattering in the sample caused by the background laser light between the femtosecond laser pulses.

3.2. Background signal analysis from Rayleigh scattering trace

The ratio of background laser energy content $W_{b,tr}$ in the time resolved regions t_{ub} to t_{pb} and t_{pe} to t_{ue} (5.4 ns) to the laser pulse and background laser energy W_{tur} in the unresolved time region t_{pb} to t_{pe} (2.9 ns) is

$$\frac{W_{b,tr}}{W_{tur}}=\frac{\int_{t_{ub}}^{t_{pb}}S_n(t)\,dt+\int_{t_{pe}}^{t_{ue}}S_n(t)\,dt}{\int_{t_{pb}}^{t_{pe}}S_n(t)\,dt}=1.35\times10^{-3}.$$

The total background energy content W_b between the femtosecond laser pulses and the average background laser power $\bar{P}_b$ or the average background laser intensity $\bar{I}_b$ are estimated in the following by assuming that the background laser power $P_b(t)$ in the unresolved time region from t_{pb} to t_{pe} is the same as in the resolved time regions from t_{ub} to t_{pb} and t_{pe} to t_{ue}. Using this assumption it is

$$\int_{t_{pb}}^{t_{pe}}S_n(t)\,dt=\kappa[W_p+(t_{pe}-t_{pb})\bar{P}_b], \tag{1}$$

and

$$\int_{t_{ub}}^{t_{pb}}S_n(t)\,dt+\int_{t_{pe}}^{t_{ue}}S_n(t)\,dt$$
$$=\kappa(t_{pb}-t_{ub}+t_{ue}-t_{pe})\bar{P}_b, \tag{2}$$

where κ is a proportionality constant and W_p is the laser pulse energy. Eq. (2) determines the average background laser power to

$$\bar{P}_b = \frac{\int_{t_{ub}}^{t_{pb}} S_n(t)\,dt + \int_{t_{pe}}^{t_{ue}} S_n(t)\,dt}{\kappa(t_{pb} - t_{ub} + t_{ue} - t_{pe})}. \quad (3)$$

The laser background energy content is

$$W_b = T\bar{P}_b, \quad (4)$$

where T is the temporal laser pulse separation (half of the resonator round-trip time). The ratio of background energy content to pulse energy is obtained from eqs. (1)–(4) to be

$$\frac{W_b}{W_p} = T\left[\int_{t_{ub}}^{t_{pb}} S_n(t)\,dt + \int_{t_{pe}}^{t_{ue}} S_n(t)\,dt\right] \times \left\{(t_{pb} - t_{ub} + t_{ue} - t_{pe}) \int_{t_{pu}}^{t_{pe}} S_n(t)\,dt - (t_{pe} - t_{pb})\left[\int_{t_{ub}}^{t_{pb}} S_n(t)\,dt + \int_{t_{ub}}^{t_{ue}} S_n(t)\,dt\right]\right\}^{-1}. \quad (5)$$

The ratio of average laser background power $\bar{P}_b$ or intensity $\bar{I}_b$ to peak laser power P_{0L} or intensity I_{0L} is

$$\frac{\bar{P}_b}{P_{0L}} = \frac{\bar{I}_b}{I_{0L}} = \frac{1}{2}\left(\frac{\pi}{\ln(2)}\right)^{1/2} \frac{\Delta t_L}{T} \frac{W_b}{W_p}. \quad (6)$$

The relation $W_p = 0.5(\pi/\ln 2)^{1/2}\Delta t_L P_{0L}$ for gaussian pulses is used in eq. (6).

The experimental data of fig. 2 give $W_b/W_p \approx 2\times10^{-3}$ (eq. (5)) and $\bar{I}_b/I_{0L} \approx 2.5\times10^{-8}$ (eq. (6)). Some contributions of the transit-time spreading of the MCP photomultiplier and of the timing jitter of the discriminators to the pedestal signal in the time range between t_{ub} to t_{pb} and t_{pe} to t_{ue} would reduce W_b/W_p and $\bar{I}_b/I_{0L}$.

It should be emphasized that in the determination of the background energy ratio W_b/W_p and in the average background intensity ratio $\bar{I}_b/I_{0L}$ it was assumed that the background intensity level in the unresolved temporal region from t_{pb} to t_{pe} is the same as in the resolved temporal region. The theoretical understanding of femtosecond pulse formation in a CPM dye laser [15–18] (background suppression in leading edge region of pulse by saturable absorber, and background suppression in trailing pulse region by partial fast absorption recovery of saturable absorber [26] combined with gain saturation of amplifying dye [23]) supports this assumption. Otherwise only an upper limit of the background intensity level in the unresolved temporal region may be determined from an analysis of the second harmonic autocorrelation traces.

3.3. Upper limit estimation of background intensity level from autocorrelation trace

In noncollinear phasematched second harmonic intensity autocorrelation measurements the normalized autocorrelation signal $S_a(\tau)/S_a(0)$ is given by [18,27]

$$\frac{S_a(\tau)}{S_a(0)} = \frac{\int_0^T I_1(t)\,I_2(t-\tau)\,dt}{\int_0^T I_1(t)\,I_2(t)\,dt}, \quad (7)$$

where τ is the temporal delay between the interacting noncollinear pulses 1 and 2.

With $I_1(t) = I_2(t) = I(t) = \bar{I}_b + I_p(t)$, eq. (7) gives

$$\frac{S_a(\tau)}{S_a(0)} = \frac{\bar{I}_b^2 T + 2I_b\int_0^T I_p(t)\,dt + \int_0^T I_p(t)I_p(t-\tau)\,dt}{\bar{I}_b^2 T + 2I_b\int_0^T I_p(t)\,dt + \int_0^T I_p^2(t)\,dt}. \quad (8)$$

Outside the pulse overlap region ($\tau \gg \Delta t_L$) the integral $\int_0^T I_p(t)\,I_p(t-\tau)\,dt$ vanishes.

Setting $\bar{I}_b = \beta I_{0L}$ and $I_p(t) = I_{0L}\exp(-t^2/t_0^2)$ ($t_0 = 0.5\,\Delta t_L[\ln(2)]^{-1/2}$) one obtains

$$\frac{S_a(\bar{\tau})}{S_a(0)} = \frac{T\beta^2 + 2\pi^{1/2}t_0\beta}{T\beta^2 + 2\pi^{1/2}t_0\beta + 2^{-1/2}\pi^{1/2}t_0}. \quad (9)$$

Solving eq. (9) to the background intensity ratio $\beta = \bar{I}_b/I_{0L}$ results in

$$\beta = \frac{\pi^{1/2}t_0}{T}\left\{-1 + \left[1 + \frac{S_a(\bar{\tau})/S_a(0)}{1 - S_a(\bar{\tau})/S_a(0)}\frac{T}{(2\pi)^{1/2}t_0}\right]^{1/2}\right\} \approx \frac{1}{2^{1/2}2}\frac{S_a(\bar{\tau})}{S_a(0)}. \quad (10)$$

The accuracy of the intensity autocorrelation traces allows an estimation of $S_a(\bar{\tau})/S_a(0) \lesssim 10^{-2}$ leading to $\beta = \bar{I}_b/I_{0L} \lesssim 3.5\times10^{-3}$.

4. Conclusions

The background energy content of a linear cw CPM dye laser was determined by Rayleigh signal analysis with an ungated inverse time-correlated single photon counting system. Assuming a constant background level for all times a background to peak pulse ratio of $\bar{I}_b/I_{0L} \approx 2.5 \times 10^{-8}$ and a background energy content of $W_b \approx 0.002\ W_p$ are obtained. The described Rayleigh scattering technique cannot exclude the possibility of a higher background level in the unresolved temporal region of the instrumental response of the detection system to the femtosecond pulses. The noncollinear second harmonic generation intensity autocorrelation trace analysis allows the estimation of an upper limit of the background to peak pulse ratio of $\bar{I}_b/I_{0L} \lesssim 3.5 \times 10^{-3}$ in the unresolved temporal region.

References

[1] G. Dube, Appl. Phys. Letters 18 (1971) 69.
[2] D. von der Linde, IEEE J. Quantum Electron. QE-8 (1972) 328.
[3] W. Seka, J. Soures, D. Lewis, J. Bunkenburg, D. Brown, S. Jacobs, G. Mourou and J. Zimmermann, Appl. Optics 19 (1980) 409.
[4] J. Boles, D.C. Brown, J. Eastman, J. Hoose, R. Hopkins, L. Iwan, S.D. Jacobs, J.H. Kelly, S. Kumpan and S. Letzring, IEEE J. Quant. Electron. QE-17 (1981) 1620.
[5] M.A. Duguay, J.W. Hansen and S.L. Shapiro, IEEE J. Quantum Electron. QE-6 (1970) 725.
[6] C.C. Wang and E.L. Baardsen, Appl. Phys. Lett. 15 (1969) 396.
[7] R.C. Eckardt and C.H. Lee, Appl. Phys. Lett. 15 (1969) 425.
[8] P.M. Rentzepis, C.J. Mitschele and A.C. Saxman, Appl. Phys. Lett. 17 (1970) 122.
[9] D.H. Auston, Appl. Phys. Lett. 18 (1971) 249.
[10] W. Leupacher and A. Penzkofer, Appl. Phys. B29 (1982) 263.
[11] G. Albrecht, A. Antonetti and G. Mourou, Optics Comm. 40 (1981) 59.
[12] D.J. Bradley, B. Liddy, A.G. Roddie, W. Sibbett and W.E. Sleat, Optics Comm. 4 (1972) 377.
[13] R.J. Harrach, T.D. MacVicar, G.I. Kachen and L.L. Steinmetz, Optics Comm. 5 (1972) 175.
[14] J. Wiedmann and A. Penzkofer, Optics Comm. 25 (1978) 226.
[15] C.V. Shank, in Ultrafast Laser Pulses and Applications, ed. W. Kaiser, Topics in Appl. Phys. Vol. 60 (Springer, Berlin, 1988) p. 5.
[16] J. Herrmann and B. Wilhelmi, Laser für ultrakurze Lichtimpulse (Physik-Verlag, Weinheim, 1984).
[17] A. Penzkofer, Appl. Phys. B 46 (1988) 43.
[18] J.C. Diels, in: Dye laser principles with applications, eds. F.J. Duarte and L.W. Hillman (Academic Press, Boston, 1990) pp. 41.
[19] D.V. O'Connor and D. Phillips, Time-correlated single photon counting (Academic Press, London, 1984).
[20] T. Murav, I. Yamazaki and K. Yoshihara, Appl. Optics 21 (1982) 2297.
[21] J.A. Valdmanis and R.L. Fork, IEEE J. Quantum Electron. QE-22 (1986) 112.
[22] W. Rudolph and B. Wilhelmi, Light pulse compression (Harwood, London, 1989).
[23] A. Penzkofer and W. Bäumler, Opt. Quantum Electron. 24 (1991) in print.
[24] A. Watanabe and S. Tanaka, H. Kobayashi, Y. Ishida and T. Yajima, Rev. Sci. Instrum. 56 (1985) 2259.
[25] Technical data sheet of Du Pont de Nemours, E-65141-2 4.85.
[26] A. Penzkofer and W. Bäumler, Opt. Quant. Electron. 23 (1991) 439.
[27] H.P. Weber, J. Appl. Phys. 38 (1966) 2231.